AUTOPHAGY
2024, VOL. 20, NO. 3, 489–504
https://doi.org/10.1080/15548627.2023.2259282

Taylor & Francis
Taylor & Francis Group

RESEARCH PAPER

FGF21 and autophagy coordinately counteract kidney disease progression during aging and obesity

Satoshi Minami, Shinsuke Sakai, Takeshi Yamamoto, Yoshitsugu Takabatake, Tomoko Namba-Hamano, Atsushi Takahashi, Jun Matsuda, Hiroaki Yonishi, Jun Nakamura, Shihomi Maeda, Sho Matsui, Isao Matsui, and Yoshitaka Isaka

Department of Nephrology, Osaka University Graduate School of Medicine, Suita, Osaka, Japan

ABSTRACT

Chronic kidney disease (CKD) has reached epidemic proportions worldwide, partly due to the increasing population of elderly and obesity. Macroautophagy/autophagy counteracts CKD progression, whereas autophagy is stagnated owing to lysosomal overburden during aging and obesity, which promotes CKD progression. Therefore, for preventing CKD progression during aging and obesity, it is important to elucidate the compensation mechanisms of autophagy stagnation. We recently showed that FGF21 (fibroblast growth factor 21), which is a prolongevity and metabolic hormone, is induced by autophagy deficiency in kidney proximal tubular epithelial cells (PTECs); however, its pathophysiological role remains uncertain. Here, we investigated the interplay between FGF21 and autophagy and the direct contribution of endogenous FGF21 in the kidney during aging and obesity using PTEC-specific *fgf21*- and/or *atg5*-deficient mice at 24 months (*aged*) or under high-fat diet (*obese*) conditions. PTEC-specific FGF21 deficiency in *young* mice increased autophagic flux due to increased demand of autophagy, whereas *fgf21*-deficient *aged* or *obese* mice exacerbated autophagy stagnation due to severer lysosomal overburden caused by aberrant autophagy. FGF21 was robustly induced by autophagy deficiency, and *aged* or *obese* PTEC-specific *fgf21*- and *atg5*-double deficient mice deteriorated renal histology compared with *atg5*-deficient mice. Mitochondrial function was severely disturbed concomitant with exacerbated oxidative stress and downregulated TFAM (transcription factor A, mitochondrial) in double-deficient mice. These results indicate that FGF21 is robustly induced by autophagy disturbance and protects against CKD progression during aging and obesity by alleviating autophagy stagnation and maintaining mitochondrial homeostasis, which will pave the way to a novel treatment for CKD.

ARTICLE HISTORY
Received 1 November 2022
Revised 8 September 2023
Accepted 11 September 2023

KEYWORDS
Ageing; autophagy stagnation; FGF21; lysosome; mitochondria; obesity

Introduction

Chronic kidney disease (CKD), represented by a persistent decrease of kidney function for over 3 months, affects more than 800 million people worldwide [1] and is one of the most common causes of death [2,3]. There are currently no curative treatments except for dialysis and kidney transplantation [4]. Importantly, the incidence of CKD continues to rise, partly due to the increasing population of elderly and obesity, which are well known risk factors for the progression of CKD [5]. Therefore, there is an urgent need to elucidate the molecular mechanism how aging and obesity progress CKD, which remains largely unknown.

Macroautophagy (hereafter referred to as autophagy) is the essential intracellular degradation system that functions to control cellular homeostasis through the quality control of proteins and organelles [6]. We have clarified that autophagy in PTECs protects them from acute kidney injury (AKI) [7] and prevents CKD progression during various chronic conditions including aging and obesity [8–11]. Conversely, we have also determined that the basal autophagic activity is higher in the kidney of age- and obesity-related CKD than that in young or control kidney. Mechanistically, various age- and obesity-related stresses increase the "demand of autophagy", defined as the amount of substrates that should be degraded by autophagy to maintain cellular homeostasis, and "autophagic flux", which is the amount of autophagic substrates that autophagy actually degrades, increases in response to the increased "demand of autophagy" in the kidney of age- and obesity-related CKD. Importantly, this increase in the "demand of autophagy" does not necessarily correlate with the "autophagic flux": the "autophagic flux" has a limit called "autophagic capacity" which is defined as the maximum amount of intracellular autophagic substrates that can be degraded by autophagy. Thus, "autophagic flux" increases in parallel with the increase in "autophagic demand" under conditions that do not exceed the limit of "autophagic capacity". Conversely, a prolonged increase in the "demand of autophagy" leads to sustained transport of autophagic substrates into lysosomes, resulting in lysosomal

CONTACT Takeshi Yamamoto tyamamoto@kid.med.osaka-u.ac.jp Department of Nephrology, Osaka University Graduate School of Medicine, Box D112-2 Yamada-oka, Suita, Osaka 585-0871, Japan
S.Minami, S.S. and T.Y. contributed equally to this work
Supplemental data for this article can be accessed online at https://doi.org/10.1080/15548627.2023.2259282

overload and dysfunction, and then leading to impaired autophagic flux [8,9,12]. In other words, "autophagic capacity" cannot keep up with increased "demand of autophagy", which in turn stagnates autophagic flux (referred to as "autophagy stagnation") [8,9,13]. We previously established the method to assess "autophagic flux" accurately *in vivo* by measuring the turnover of autophagosomes using GFP-MAP1LC3B (microtubule-associated protein 1 light chain 3 beta) transgenic mice and lysosomal inhibitors [8], and we also developed the method to evaluate the "demand of autophagy" by quantifying the accumulation of autophagic substrates such as SQSTM1/p62- and ubiquitin-positive protein aggregates when autophagy is genetically or pharmacologically disrupted [14]. To be clinically important, it has recently been reported that the increased "demand of autophagy" are closely associated with the pathogeneses of Alzheimer disease: a prolonged increase in the "demand of autophagy" leads to autophagy stagnation due to lysosomal overload, which exacerbates the pathogenesis of the disease [12]. In age- and obesity-related CKD, further autophagic activation that would normally be induced when the kidney is subjected to additional stresses, including ischemia, cannot be induced due to autophagy stagnation caused by a prolonged increase in the "demand of autophagy" [8,9]. Thus, the autophagy stagnation could contribute to the vulnerability to AKI in elderly and obese patients. We have further revealed that the autophagy stagnation is recapitulated in human patients of age- and obesity-related CKD [9,15]. Based on these findings, the autophagic stagnation could be one of the common underlying molecular mechanisms that promotes CKD progression during aging and obesity. Therefore, it is important to elucidate the molecular mechanisms that stagnate autophagy as well as to clarify the intracellular compensation mechanisms against the autophagy stagnation for preventing CKD progression during aging and obesity.

FGF21 (fibroblast growth factor 21), a hormone-like member of FGF family, has proven to control metabolic multi-organ crosstalk enhancing energy expenditure through glucose and lipid metabolism [16]. FGF21 is mainly expressed in several metabolically active tissue organs, such as the liver, adipose tissue, and pancreas [17]. Recent reports elucidated that FGF21 have protective roles against age- and obesity-related disorders. FGF21 acts as a stress hormone induced in response to diverse pathogenic conditions in several mammalian tissues, including the liver [18,19], skeletal muscle [20,21] and heart [22], and protects against various age- and obesity-related disorders [23–25]. Furthermore, transgenic overexpression of FGF21 markedly extends lifespan in mice [26]. Most interestingly, recent analyses revealed the close relationship between FGF21 and autophagy; skeletal muscle-specific autophagy deficiency significantly induced FGF21 secretion from skeletal muscle, which protects against diet-induced obesity and insulin resistance [21], implying that FGF21 could be a clue to elucidate the compensatation mechanism of autophagic stagnation during aging and obesity.

In recent years, the relationship between FGF21 and the kidney has been extensively studied, and there is ample evidence that administration of exogenous FGF21 ameliorates hyperlipidemia- or diabetes- induced kidney injury, mainly by improving systemic metabolic alterations in mice [27,28]. Recently, we have for the first time revealed that FGF21 is expressed normally at a very low level but this becomes increased during prolonged starvation in kidney PTECs, especially in autophagy-deficient PTECs [29]. The research from the other groups verified that FGF21 is induced in the kidney during diabetic kidney disease and cisplatin-induced AKI [30,31]. However, the direct contribution of endogenous FGF21 secreted locally from PTECs to kidney function has not been investigated yet, although our understanding of the systemic effects of exogenous or endocrine FGF21 is exponentially increasing.

Based on this background information, in the present study, we investigated 1) the direct contribution of endogenous FGF21 in the kidney and 2) the possible interplay between FGF21 and autophagy in the progression of CKD during aging and obesity.

Results

FGF21 deficiency induces tubular injury, enlarged lysosomes, and SQSTM1/p62 accumulation in the PTECs of aged and obese mice

To evaluate the effect of FGF21 deficiency in PTECs, we crossed the *Kap* (kidney androgen regulated protein)-Cre transgenic mice with mice bearing an $Fgf21^{flox}$ allele and generated *fgf21*-floxed *Kap*-Cre mice ($fgf21^{F/F}$-TSKO [tissue-specific knockout]). There was no significant histological difference in the kidney between $fgf21^{F/F}$-TSKO and CTRL (control) mice at 2-months of age (Figure S1A). We followed these mice up to 24 months (hereafter, young refers to 2-months of age and aged to 24 months of age). Biochemical and physiological parameters are shown in Table S1. There were no changes in plasma FGF21 concentration and metabolic profiles between aged CTRL and $fgf21^{F/F}$-TSKO mice, indicating that FGF21 produced in PTECs has no effect on plasma FGF21 concentration and systemic metabolism. Periodic-acid Schiff (PAS) staining demonstrated that the kidneys from *aged* $fgf21^{F/F}$-TSKO mice showed more severe tubular injury such as multiple cytosolic vacuolar formation, tubular lumen dilation and tubular atrophy, which was hardly observed in aged CTRL mice (Figure 1A). Consistently, the expression of tubular damage markers such as *Havcr1/Kim-1* and *Lcn2/Ngal* tended to be upregulated in aged $fgf21^{F/F}$-TSKO mice (Figure S1B and S1C). As for tubular cytosolic vacuoles in *aged* $fgf21^{F/F}$-TSKO mice, the margins of the vacuoles were surrounded by the lysosomal transmembrane protein, LAMP1 (Figure 1A). Electron microscopy analysis revealed that aged $fgf21^{F/F}$-TSKO mice showed enlarged lysosomes containing undigested materials and lipids in PTECs (Figure 1B). Furthermore, we found massive accumulation of SQSTM1/p62 (sequestosome 1), which is the ubiquitin- and MAP1LC3-binding protein removed by autophagy, thus serving as an index of autophagic degradation, in the kidneys of aged $fgf21^{F/F}$-TSKO mice (Figure 1C), even though mRNA

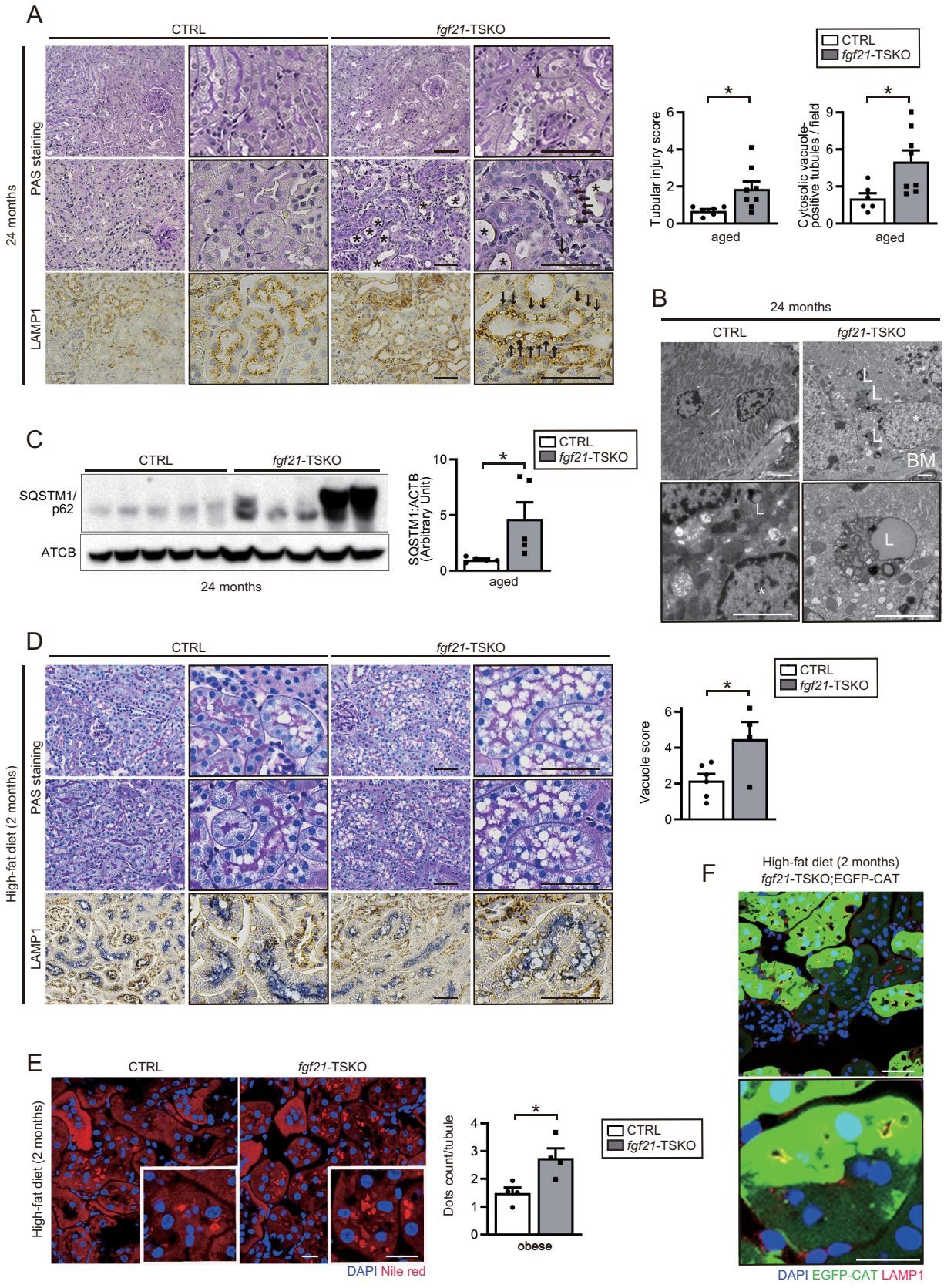

Figure 1. FGF21 deficiency induces tubular injury, enlarged lysosomes, and SQSTM1/p62 accumulation in the PTECs of *aged* and *obese* mice. (A) Representative images of PAS staining and LAMP1 immunostaining of the kidney cortical regions of *aged* CTRL and *fgf21*$^{F/F}$-TSKO mice ($n = 6$ to 8). Kidney sections were counterstained with hematoxylin. Arrows indicate cytosolic vacuolar formation, and asterisks indicate atrophic tubules with lumenal dilatation. (A right) the tubular injury score was shown, and the number of cytosolic vacuole-positive tubules was counted in at least 10 high-power fields (×400) (B) electron micrographs of the kidneys of *aged* CTRL and *fgf21*$^{F/F}$-TSKO mice ($n = 3$). Magnified images of lysosomes are presented. BM, basement membrane; L, lysosomes; TL, tubular lumen; *, nucleus. (C) Representative immunoblot and quantification by densitometry of the protein level of SQSTM1/p62 using whole kidney lysates of *aged* CTRL and *fgf215*$^{F/F}$-TSKO mice are shown ($n = 5$). ACTB was used as loading control. (D) Representative images of PAS staining and LAMP1 immunostaining in the kidney cortical

level was unchanged (Figure S1D), suggesting that FGF21 deficiency disrupted autophagic flux in the aged kidneys. No obvious exacerbation in interstitial fibrosis or inflammation in the kidney was observed in aged *fgf21*$^{F/F}$-TSKO mice (Figure S1E, S1F, S1G, and S1H). Consistently, there were also no significant differences in renal function such as plasma creatinine, cystatin C levels and urinary albumin excretion between aged CTRL and *fgf21*$^{F/F}$-TSKO mice (Table S1).

Inspired by our recent research that a high-fat diet (HFD) induces enlarged lysosomes accumulating phospholipids in PTECs [9], young *Fgf21*$^{F/F}$-CTRL and *fgf21*$^{F/F}$-TSKO mice were fed a HFD for 2 months (hereafter, referred to as obese). As previously reported, HFD induced formation of cytosolic vacuoles in PTECs of CTRL mice, most of which were margined with LAMP1 and positively stained with Nile red, which can detect phospholipids. LAMP1-positive cytosolic vacuolar formation and the phospholipid accumulation was significantly exacerbated in *obese fgf21*$^{F/F}$-TSKO mice compared with obese CTRL mice (Figures 1D, 1E). Furthermore, to examine whether FGF21 deficiency leads to enlarged lysosomes in a cell-intrinsic manner, we crossed *fgf21*$^{F/F}$-TSKO mice with EGFP (enhanced green fluorescent protein)-chloramphenicol acetyltransferase (ChAT) transgenic mice, in which EGFP can be detected only after Cre-mediated recombination [32]. Greater number of LAMP1-margined cytosolic vacuoles was observed in EGFP positive PTECs than in EGFP negative PTECs (Figure 1F).

Autophagic flux is increased by FGF21 deficiency in the PTECs of young mice

Next, to evaluate how basal and starvation-induced autophagic flux is altered by FGF21 deficiency in *young* mice, we crossed *Fgf21*$^{F/F}$ (*Fgf21*$^{F/F}$-CTRL) or *fgf21*$^{F/F}$-TSKO mice with GFP-MAP1LC3B transgenic mice. Chloroquine, an inhibitor of intralysosomal acidification, was administered 6 h before euthanasia and the number of GFP-positive puncta (which represent autophagosomes) was compared with and without chloroquine administration. Upon 24 h of starvation, chloroquine administration did not significantly increase the number of puncta in the PTECs of young CTRL mice, while the increase was significant in young *fgf21*$^{F/F}$-TSKO mice. These results indicate that, in contrast to aged *fgf21*$^{F/F}$-TSKO mice, autophagic flux is increased in the PTECs of young *fgf21*$^{F/F}$-TSKO mice (Figure 2A,B).

To explore the possible cellular mechanisms of the FGF21 deficiency-mediated increase in autophagic flux of young mice, we investigated the key signaling pathways that modulate autophagy, AMP-activated protein kinase (AMPK) and MTOR (mechanistic target of rapamycin kinase) complex 1 (MTORC1). Western blot analysis using whole kidney lysates demonstrated that the levels of phosphorylated PRKAA/AMPK and phosphorylated RPS6 (ribosomal protein S6), downstream of MTORC1 were unchanged (Figure S2). Collectively, in *fgf21*$^{F/F}$-TSKO mice, autophagy is activated in an AMPK- and MTOR-independent manner in young age, while autophagy is impaired with accumulation of undigested materials within enlarged lysosomes in aging.

FGF21 deficiency increases the demand of autophagy leading to lysosomal overburden in the PTECs of aged and obese kidney

The above results led us to infer that FGF21 deficiency may increase the demand of autophagy, because previous report has elucidated that short-term accumulation of autophagic substrates upregulates autophagic flux whereas sustained overload of autophagic substrate impairs autophagic flux due to lysosomal overburden [12]. Therefore, we infer that FGF21 deficiency may increase the demand of autophagy and evaluated FGF21-mediated changes in the demand of basal and starvation-induced autophagy by comparing the accumulation of autophagic substrates between young PTEC-specific *atg5*-deficient (*atg5*$^{F/F}$- TSKO mice) and young PTEC-specific *fgf21*- and *atg5*-deficient mice (*fgf21*$^{F/F}$*atg5*$^{F/F}$-TS double KO [TSDKO] mice). As expected, the accumulation of autophagic substrates (assessed by SQSTM1/p62- and ubiquitin-positive protein aggregates) was significantly increased in the PTECs of starved TSDKO mice than in starved *atg5*$^{F/F}$- TSKO mice (Figures 3A,B), indicating that FGF21 deficiency increases the demand of autophagy. Next, to investigate whether the enlarged lysosomes under FGF21 deficiency is actually due to aberrant autophagy, we compared the lysosomal morphology in the PTECs of obese CTRL, *fgf21*$^{F/F}$-TSKO and TSDKO mice under a HFD for 2 months by assessing PAS and LAMP1 staining. We observed marked suppression of HFD-induced enlarged lysosomes in the PTECs of TSDKO mice compared with *fgf21*$^{F/F}$-TSKO mice (Figure 4A,B). Collectively, these results indicate that FGF21 deficiency increases the demand of autophagy, leading to the increased autophagic flux in *young* mice while it can stagnate autophagy in *aged* and *obese* mice due to lysosomal overburden.

FGF21 deficiency accelerates kidney aging in autophagy-deficient mice

Next, we investigated whether FGF21 is secreted from autophagy-deficient PTECs in aged kidneys, as in the case of prolonged starvation [29], by measuring the samples of the aged *atg5*-TSKO and CTRL mice previously reported [8]. *Fgf21* mRNA level was significantly increased in the isolated PTECs of aged *atg5*-TSKO mice compared with young *atg5*-TSKO mice and *aged* CTRL littermates (Figure 5A). The plasma FGF21 concentration was higher in aged mice compared with young mice, while it was

regions of *obese* CTRL and *fgf21*$^{F/F}$-TSKO mice ($n = 4$–6). Kidney sections were counterstained with hematoxylin and immunostained for the proximal tubule marker LRP2/MEGALIN in blue. (D right) the vacuole score was shown. (E) Representative images of Nile red staining in the kidney cortical regions of *obese* CTRL and *fgf21*$^{F/F}$-TSKO mice ($n = 4$). The number of Nile red-positive puncta per proximal tubule was counted in at least 10 high-power fields (×600). (F) Representative fluorescent images of the kidney cortical regions of *obese fgf21*$^{F/F}$-TSKO;EGFP-ChAT mice ($n = 4$). Kidney sections were immunostained for LAMP1 (red) and counterstained with DAPI (blue). (D to F) *obese* mice were fed a high-fat diet for 2 months. Bars: 50 m (A and D), 2 m (B) and 20 m (E and F). Data are expressed as the fold change relative to the mean value of *aged* (C) or *obese* (E) CTRL mice and are provided as means ± SE. Statistically significant differences (*$P < 0.05$) are indicated.

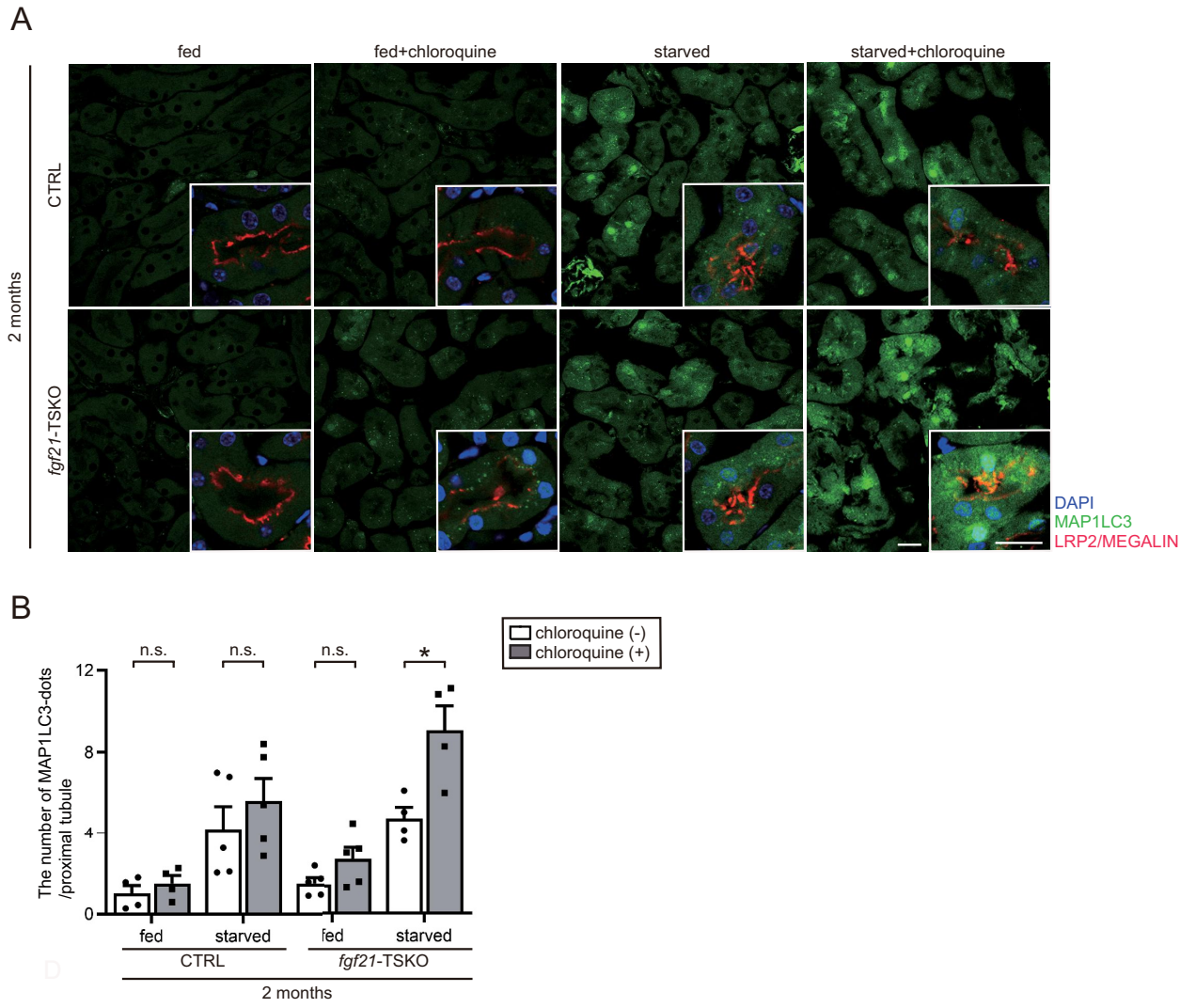

Figure 2. Autophagic flux is increased by FGF21 deficiency in PTECs of *young* mice. (A and B) *in vivo* evaluation of the autophagic flux in PTECs of young mice. (A) Representative fluorescent images of the kidney cortical regions of young CTRL;GFP-MAP1LC3B and *fgf21*$^{F/F}$-TSKO;GFP-MAP1LC3B mice that were either fed or subjected to 24 hours of starvation, with or without chloroquine administration ($n = 4$ to 5). Kidney sections were immunostained for LRP2/MEGALIN, a marker of proximal tubules (red), and counterstained with DAPI (blue). Magnified images are presented in the insets. Bars: 20 m. (B) the number of GFP-positive puncta per proximal tubule under each condition was counted in at least 10 high-power fields (×600). Data are provided as means ± SE. Statistically significant differences (*$P < 0.05$) are indicated.

comparable between aged *atg5*-TSKO mice and aged CTRL littermates (Figure S3A). To examine whether increased secretion of FGF21 from the kidney of aged *atg5*-TSKO mice protects the kidney against aging stress, we followed TSDKO mice up to 24 months, and compared the aging phenotypes, especially with aged *atg5*$^{F/F}$-TSKO mice. The significant increase in *Fgf21* expression in the kidney of aged *atg5*-TSKO mice was almost completely abolished in the kidney of aged TSDKO mice (Figure 5B). Biochemical and physiological parameters are shown in Table 1. There were no significant differences in most parameters among these mice, whereas the body weight was lowered in *aged atg5*-TSKO mice compared with aged CTRL. The mRNA levels of tubular injury markers *Havcr1/Kim-1* was increased in aged TSDKO mice compared with aged CTRL and *atg5*-TSKO mice (Figure 5C). The proximal tubules of *aged* TSDKO showed exaggerated tubular injuries (such as brush border loss, disruption of lumen structure, and cast formation), as well as a massive accumulation of cytosolic amorphous substrates compared with aged *atg5*-TSKO mice (Figure 5D). Furthermore, *aged* TSDKO mice exhibited enhanced interstitial fibrosis as assessed by COL1A1 (collagen, type I, alpha 1) immunostaining, *Col1a1* and *Tgfb* mRNA, Masson trichrome staining, and Sirius red staining (Figure 5E–H) and patchy ADGRE1/F4/80-positive macrophage infiltration into the outer stripe of the outer medulla (Figure 5I). In recent years, cellular senescence has emerged as an important driver of aging and age-related disease in multiple organs including the kidney [33]. Messenger RNA levels of *Cdkn2a/p19*^{Arf} (*cyclin dependent kinase inhibitor 2A*) and immunostaining for CDKN1A/p21^{cip1} (cyclin dependent kinase inhibitor 1A) and phospho-H2AFX/γ-H2AX (H2A. X variant histone), demonstrated that cellular senescence was exaggerated in the PTECs of aged TSDKO mice (Figure S3B, S3C and S3D).

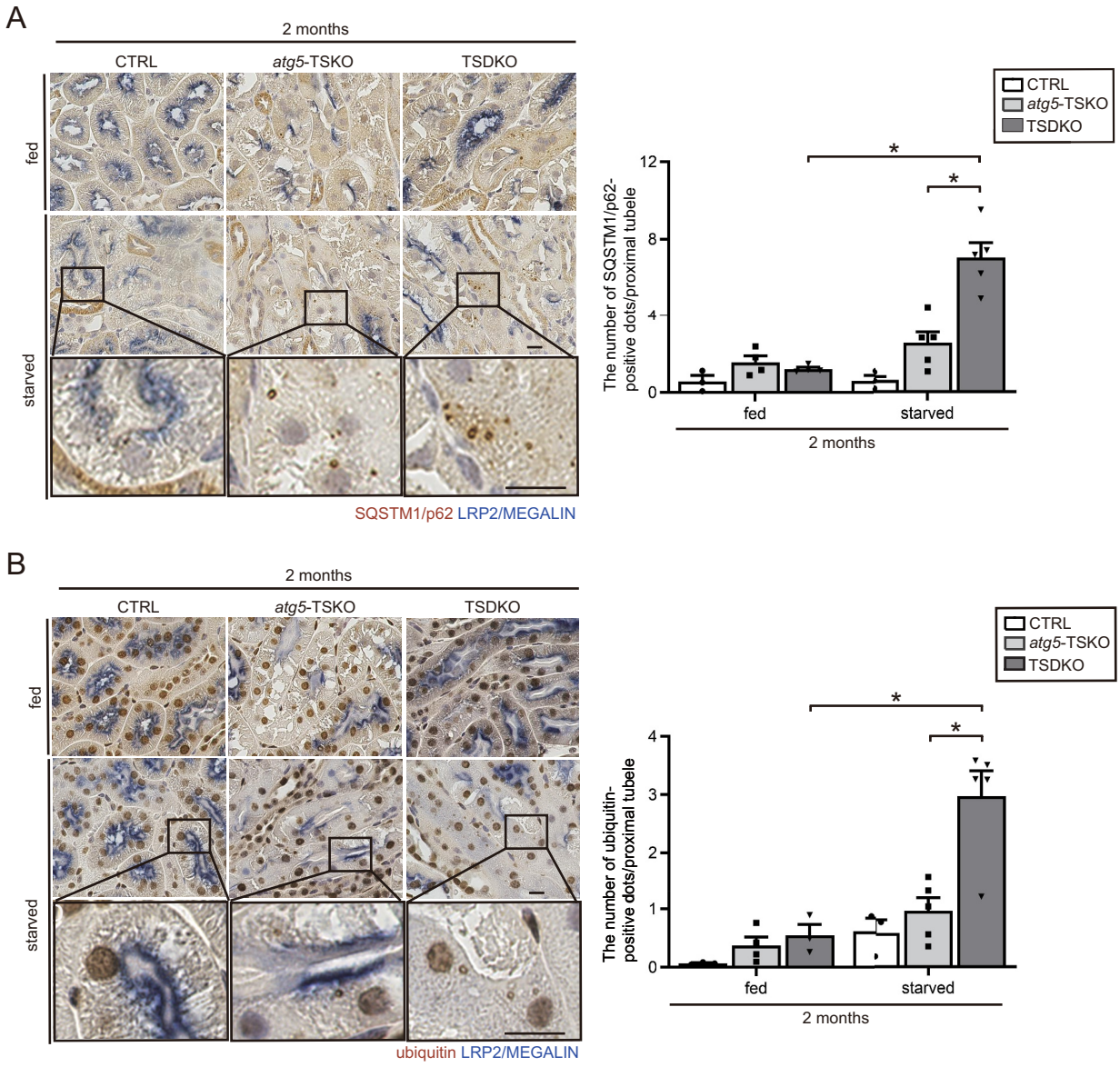

Figure 3. *Fgf21*-deficient PTECs are more reliant on autophagy for the degradation of increasing substrates. (A and B) Representative images of immunostaining for SQSTM1/p62 (A) and ubiquitin (B) in the kidney cortical regions of young CTRL, *atg5*$^{F/F}$-TSKO, and TSDKO mice that were either fed or subjected to 48 hours of starvation ($n = 3$ to 5). Magnified images are presented in the insets. The number of SQSTM1/p62- or ubiquitin-positive dots was counted in at least 10 high-power fields (×400). Kidney sections were counterstained with hematoxylin and immunostained for the proximal tubule marker LRP2/MEGALIN in blue. Bars: 10 m. Data are provided as means ± SE. Statistically significant differences (*$P < 0.05$) are indicated.

FGF21 deficiency aggravates HFD-induced kidney injury in autophagy-deficient mice

We next examined the role of FGF21 in PTECs against HFD-induced kidney injury. Consistent with aging, *Fgf21* mRNA level was significantly increased in the kidney of *atg5*-TSKO mice compared with CTRL littermates under a HFD for 2 months (Figure 6A). Then, we assessed kidney histology in *Fgf21*$^{F/F}$-CTRL, *atg5*$^{F/F}$-TSKO, and TSDKO mice which were fed a HFD for 10 months. We observed marked exacerbation of kidney injury (Figure 6B), renal fibrosis (Figure 6C,D), and inflammation (Figure 6E) in *obese* TSDKO mice.

FGF21 deficiency accelerates kidney aging with mitochondrial dysfunction and oxidative stress

Finally, we investigated the mechanism for a protective role of FGF21 against kidney disease progression. As mitochondrial dysfunction and endoplasmic reticulum (ER) stress play central roles in the progression of kidney disease [34,35], we examined the mitochondrial function and ER stress response in aged TSDKO mice. Although we could not find any difference in ER stress response among aged CTRL, *atg5*-TSKO, and TSDKO mice (Figure S4), mitochondrial function (assessed by COX [cytochrome c oxidase] and SDH [succinate dehydrogenase] staining) was significantly deteriorated in the

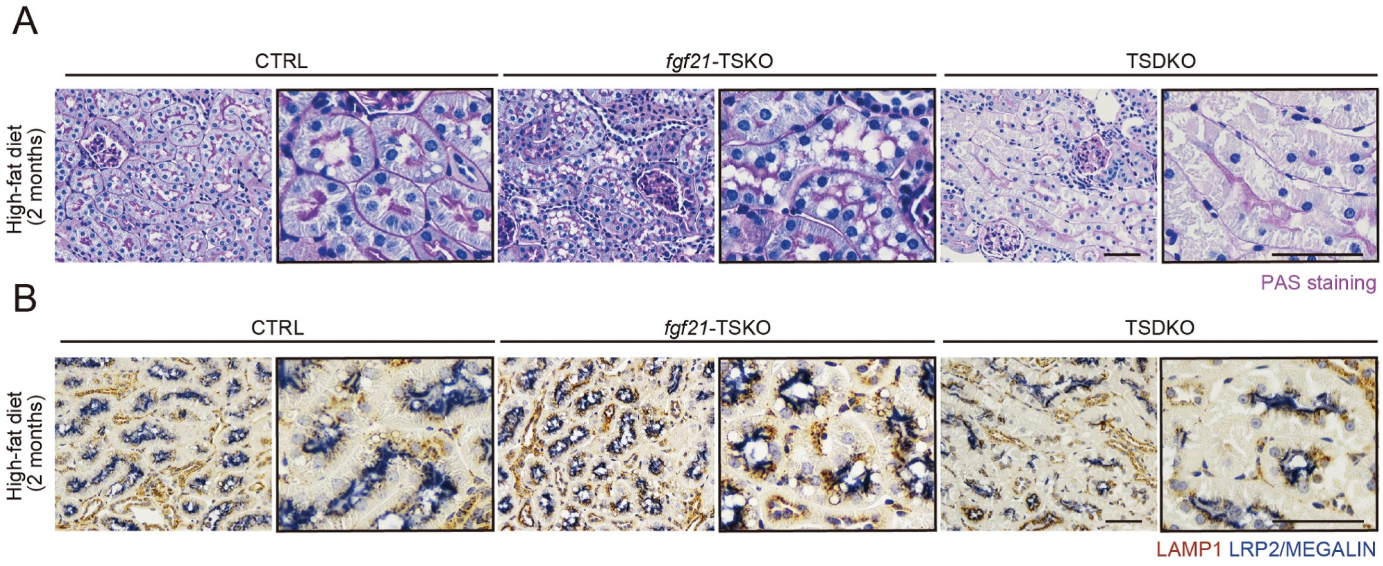

Figure 4. FGF21 deficiency induces enlarged lysosomes dependent on autophagy in the kidney of *obese* mice. (A and B) Representative images of PAS staining (A) and LAMP1 immunostaining (B) in the kidney cortical regions of obese CTRL, *fgf21*$^{F/F}$-TSKO, and TSDKO mice under a high-fat diet for 2 months ($n = 4$ to 6). Kidney sections were counterstained with hematoxylin (A and B) and immunostained for the proximal tubule marker LRP2/MEGALIN in blue (B). Bars: 50 µm.

kidneys of aged TSDKO mice compaired with *aged* CTRL and *atg5*-TSKO mice (Figure 7A). Mitochondrial dysfunction is known to be closely associated with the progression of kidney aging and lipotoxicity via the production of reactive oxygen species (ROS) [34]. Therefore, we assessed ROS production by oxidative stress markers, including dityrosine, 4-hydroxy-2-nonenal (HNE) and N-carboxymethyllysine (CML) staining and observed that increased ROS significantly in *aged* TSDKO mise kidneys (Figure 7B, S5A, and S5B). Finally, we investigated the possible mechanisms of the FGF21-mediated maintenance of mitochondrial integrity. It has been reported that FGF21 regulates the activities of SIRT1 (sirtuin 1; NAD^+ [nicotinamide adenine dinucleotide]-dependent deacetylase), PPARGC1A/PGC1A (peroxisome proliferative -activated receptor, gamma, coactivator 1 alpha) and TFAM (transcription factor A, mitochondrial), which are closely related to mitochondrial integrity [36–39], therefore, we examined the expression of these molecules. The results showed that mRNA expression level of *Tfam* (Figure 7C) and the protein levels of SIRT1, PPARGC1A/PGC1A (Figure 7D) and were significantly decreased in the kidneys of aged TSDKO mice. The expression of NAMPT (nicotinamide phosphoribosyltransferase), the rate-limiting enzyme for NAD^+ production essential for SIRT1 activation, was also markedly decreased in the kidneys of aged TSDKO mice (Figure 7D). Conversely, the activity of AMPK, which is important for activation of NAMPT and SIRT1 [40], was rather activated in the kidney of aged TSDKO mice (Figure S5C).

Discussion

In this study, we demonstrated that FGF21 is robustly induced by autophagy deficiency and acts in an autocrine and/or paracrine manner to protect against CKD progression during aging and obesity, notably characterized by tubular injury, inflammation, and fibrosis. Mechanistically, efficacy of FGF21 secretion from PTECs is not due to an improvement of the systemic metabolic alterations, but rather based on multifaceted cell-intrinsic and autophagy-related mechanisms; FGF21 alleviates lysosomal overburden by reducing the demand of autophagy and thus suppressing aberrant autophagy, and maintains mitochondrial homeostasis. A simple schematic drawing is shown in Figure 8A.

Our *in vivo* experiments using PTEC-specific *fgf21* and/or *atg5*-deficient mice clearly denoted an apparent interaction between FGF21 and autophagy in the control of CKD progression during aging and obesity; FGF21 deficiency increases the demand of autophagy, leading to compensatory enhanced autophagic flux in young mice, while stagnating autophagy in aged and obese mice due to lysosomal overburden (Figure 8B). Conversely, autophagy deficiency induces FGF21 secretion, which exerts marked protective effects against age- and obesity-related CKD progression in an autocrine/paracrine manner. The combination of their deficiency culminates in the significant deterioration of tubular injury, inflammation and fibrosis.

In the present study, we revealed a close interaction between autophagic stagnation and FGF21 in PTECs during aging and obesity. Meanwhile, what is the molecular mechanism underlying this interaction? As for the mechanism by which FGF21 is induced by autophagy stagnation in PTECs during aging and obesity, we speculate that once autophagy stagnation occurs in the PTECs, mitochondrial damage is exacerbated by the inability to properly remove damaged mitochondria, and the subsequent mitochondrial integrated stress response (mitoISR) induces FGF21. It has been reported that mitoISRs are activated when mitochondria are damaged in vivo, resulting in various adaptive responses to mitochondrial stress, and that FGF21 secretion is a representative stress response among mitoISRs that initiates even when mitochondria are mildly damaged [41]. Indeed, analysis of muscle-specific *atg7*-deficient mice has reported that autophagy

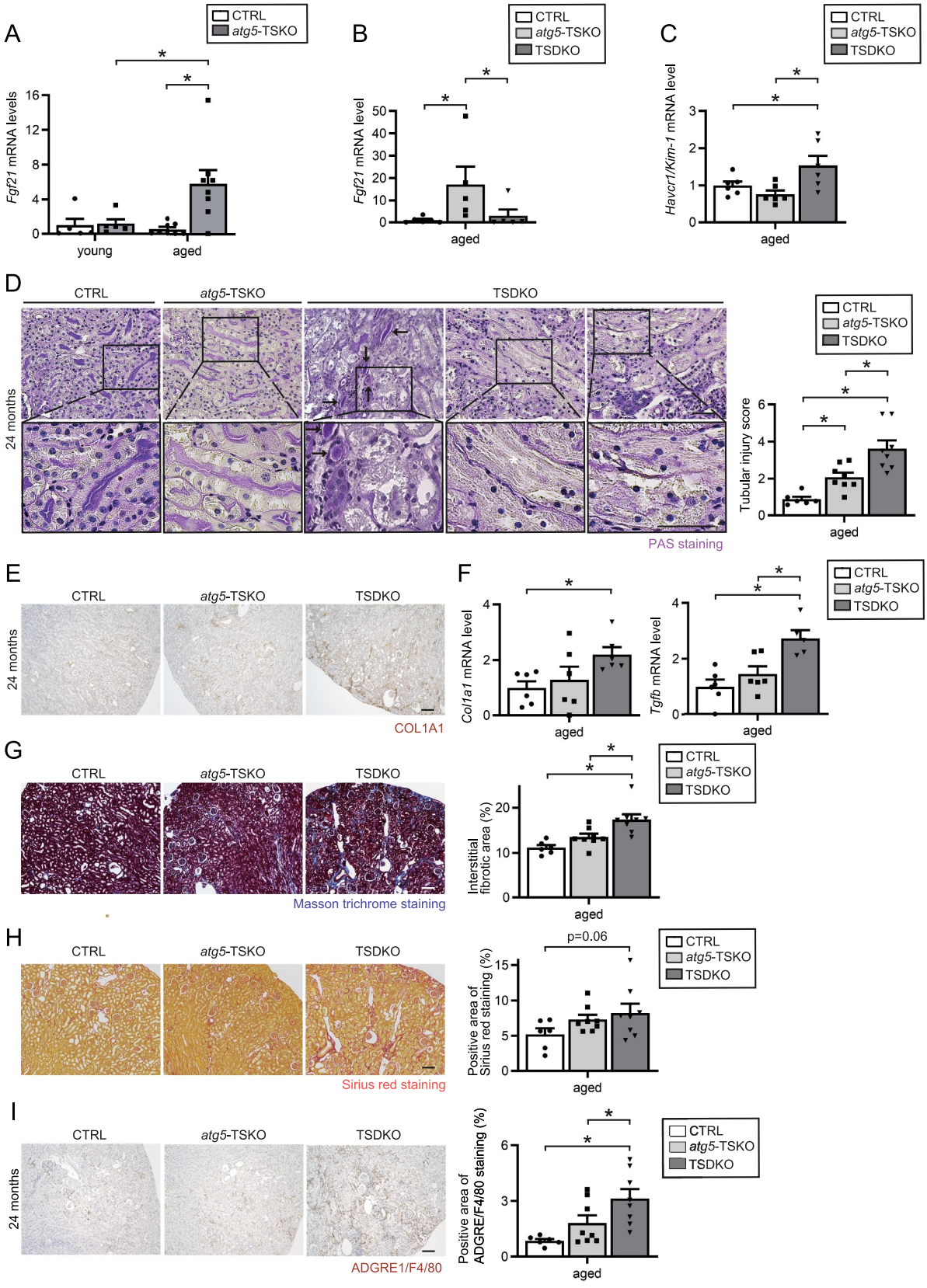

Figure 5. FGF21 deficiency accelerates kidney aging in autophagy-deficient mice. (A) mRNA expression levels of *Fgf21* using the isolated PTECs of *aged* CTRL and *atg5*$^{F/F}$-TSKO mice ($n = 5$ to 8). (B, C and F) mRNA expression levels of *Fgf21* (B), *Havcr1/Kim-1* (C), and *Col1a1* and *Tgfβ* (F) using whole kidney lysates of aged CTRL, *atg5*$^{F/F}$-TSKO, and TSDKO mice ($n = 5$ to 6). Data were normalized with *Gapdh* mRNA and presented as the ratio relative to aged CTRL kidney. (D, E, and G to I) Representative images of PAS staining (D), immunostaining for COL1A1 (E), Masson trichrome staining (G), Sirius red staining (H) and immunostaining of ADGRE1/F4/80 (I) in the kidney cortical regions of aged CTRL, *atg5*$^{F/F}$-TSKO, and TSDKO mice ($n = 6$–8). (D) Magnified images from aged CTRL, *atg5*$^{F/F}$-TSKO and TSDKO mice indicate brush border loss as well as disruption of lumen structure in the PTECs of TSDKO mice. Arrows indicate cast formation. The tubular injury score (D right), the interstitial fibrotic area (G right), Sirius red-positive area (H right) and ADGRE1/F4/80-positive area (I right) were quantified in at least 10 high-power fields (×400), respectively. (E, G and I) kidney sections were counterstained with hematoxylin. Bars: 50 m. Data are provided as means ± SE. Statistically significant differences (*$P < 0.05$) are indicated.

Table 1. Biochemical and physiological parameters of aged (24 months old) CTRL, *atg5*$^{F/F}$-TSKO, and TSDKO mice.

	CTRL	*atg5*$^{F/F}$-TSKO	TSDKO
Number of animals (at study entry)	8	11	10
Number of deaths	2	3	2
Tumor	0	0	1
Body weight (g)	43.3 ± 3.4	32.6 ± 3.0[a]	36.2 ± 3.0
Heart weight/BW (mg/g)	4.37 ± 0.38	4.61 ± 0.33	4.91 ± 0.33
Lung weight/BW (mg/g)	5.21 ± 0.62	7.17 ± 0.54 [a]	6.33 ± 0.54
Liver weight/BW (mg/g)	41.1 ± 2.5	47.5 ± 2.1	49.2 ± 2.1 [a]
Left kidney weight/BW (mg/g)	5.25 ± 0.44	5.54 ± 0.38	6.01 ± 0.38
Mesenteric adipose tissue/BW (mg/g)	11.43 ± 1.80	9.67 ± 1.56	8.63 ± 1.56
Epididymal adipose tissue/BW (mg/g)	41.7 ± 5.9	25.4 ± 5.1	30.5 ± 5.1
Brown adipose tissue/BW (mg/g)	6.62 ± 0.70	5.65 ± 0.61	6.23 ± 0.61
Soleus muscle/BW (mg/g)	0.29 ± 0.04	0.36 ± 0.03	0.38 ± 0.03
Urea nitrogen (mmol/L)	24.1 ± 1.5	23.0 ± 1.3	22.0 ± 1.3
Creatinine (mol/L)	52.5 ± 21.2	54.9 ± 18.4	32.0 ± 18.4
Cystatin C (mg/L)	1.13 ± 0.41	1.88 ± 0.33	1.15 ± 0.33
Urinary albumin/creatinine (g/gCr)	0.26 ± 0.12	0.32 ± 0.10	0.25 ± 0.10
Glucose (mmol/L)	8.23 ± 1.25	7.22 ± 0.94	7.37 ± 0.94
FGF21 (pg/mL)	548 ± 179	417 ± 155	369 ± 155
Total cholesterol (mmol/L)	2.30 ± 0.16	2.01 ± 0.14	2.24 ± 0.14
Triglyceride (mmol/L)	1.82 ± 0.34	1.13 ± 0.29	1.84 ± 0.29
Free fatty acids (mmol/L)	0.71 ± 0.13	0.44 ± 0.11	0.48 ± 0.11
Phospholipids (mmol/L)	3.59 ± 0.34	2.85 ± 0.30	3.30 ± 0.30

Biochemical and physiological parameters were analyzed in *aged* CTRL, *atg5*$^{F/F}$-TSKO, and TSDKO mice ($n = 6–8$). Values represent the mean ± SE. Statistically significant differences (a: $P < 0.05$ vs CTRL, b: $P < 0.05$ vs *atg5*$^{F/F}$-TSKO) are indicated.

failure induces FGF21 [21]. The induction of FGF21 is regulated by ATF4 (activating transcription factor 4), which is activated by mitoISR [21]. Considering that mitochondrial damage is exacerbated by failure of mitophagy in autophagy-deficient PTECs during aging (Figure 7) and obesity [9], autophagy stagnation that occurs during aging and obesity is also thought to induce FGF21 via the mitochondrial dysfunction-mitoISR-Atf4 axis. The next question about the mechanism that regulates these interactions is how FGF21 regulate the demand of autophagy in PTECs during aging and obesity. Although the mechanism by which FGF21 regulates the demand of autophagy remains unclear, one hypothesis is that the FGF21-TFAM signaling axis protects mitochondria, thereby reducing mitochondrial damage and decreasing the demand of autophagy. At the basal level, the kidney has been reported to be the organ with the highest mitochondrial selective autophagy (mitophagy) activity, which selectively removes damaged mitochondria [42]. It has also been shown that a decrease in TFAM in the kidney tubules leads to significant mitochondrial damage [43,44]. Taken together with the finding in this study that FGF21 regulates TFAM expression, it is likely that FGF21 induction reduces the demand of mitophagy by increasing TFAM expression and suppressing mitochondrial damage, while FGF21 deficiency increases the demand of mitophagy due to the accumulation of damaged mitochondria caused by reduced TFAM expression.

Recently, the idea of "FGF21 resistance" has been suggested and thought to contribute to the pathology of age- and obesity-related diseases as circulating FGF21 levels are increased under conditions such as aging, obesity and diabetes, despite the prolongevity and metabolic health-promoting effects of FGF21 [45–48]. Moreover, "autophagy stagnation" has been known to exist in CKD progression during aging and obesity [8,9,13]. Therefore, most importantly, although our findings come from the observation in genetically manipulated mice models, we believe that our *in vivo* experiments using PTEC-specific *fgf21* and/or *atg5*-deficient mice nicely reproduce clinical settings of elderly and/or obese CKD patients. Interestingly, autophagy stagnation can lead to inflammaging [49], whereas inflammaging can provoke "FGF21 resistance" and thus disturb physiological homeositasis in several tissues [23]. Although it remains to be solved whether FGF21 resistance can be developed in the elderly or obese CKD patients, a vicious cycle of "stagnation of autophagy – inflammaging - FGF21 resistance" might be created during CKD progression. Consistently, circulating FGF21 levels rise progressively with the decline of kidney function, reaching 8–15 times normal values in end stage kidney disease [50], and higher FGF21 levels correlate with poorer metabolic profile, higher inflammatory markers, more rapid decline of kidney function, and higher mortality in CKD patients [51–53]. In this regard, the present data provide insights into the pathophysiology of CKD progression during aging and obesity, and the previously unappreciated roles of endogenous FGF21 with clinical relevance.

It has been demonstrated that exogenous FGF21 treatment or FGF21 overexpression exhibits protective effects by enhancing autophagic flux [54–57]. Conversely, we found that FGF21 deficiency also increases autophagic flux in young mice, and *fgf21*-deficient PTECs are more reliant on autophagy for the degradation of increasing substrates. Although these counterintuitive findings may ultimately be reconciled by a better understanding of the intrinsically complicated biology of FGF21, these discrepant effects of FGF21 on autophagy may reflect the difference in its concentration, its diverse metabolic functions in multiple target organs, and its ability to act as an autocrine, paracrine, and endocrine factor. Exogenous administration of FGF21 or FGF21 overexpression can activate autophagy induction by modulating several signaling pathways including SIRT1 [58]

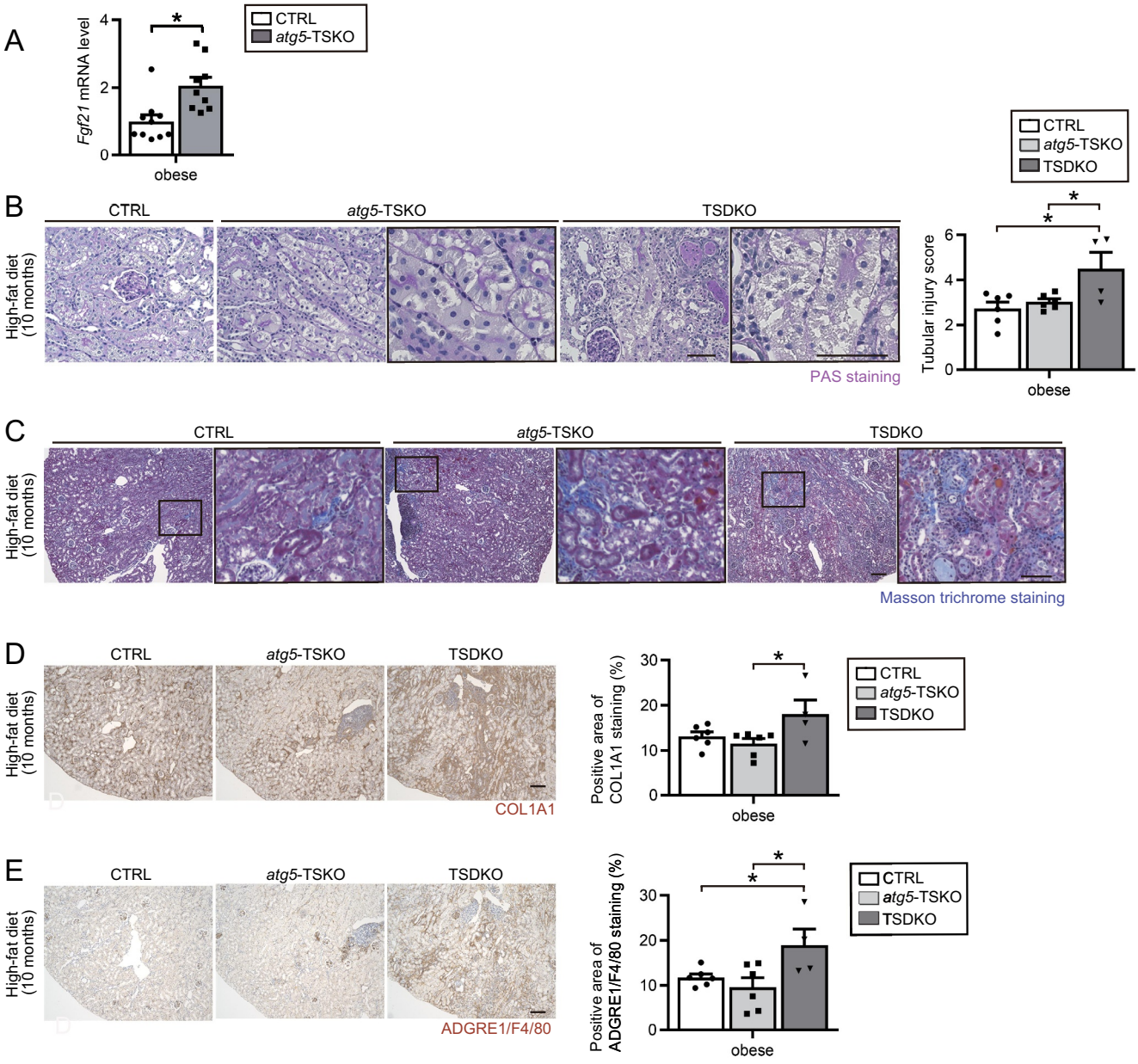

Figure 6. FGF21 deficiency aggeravates high-fat diet-induced kidney injury in autophagy-deficient mice. (A) mRNA expression levels of *Fgf21* using whole kidney lysates of obese CTRL and *atg5*$^{F/F}$-TSKO mice under a high-fat diet for 2 months ($n = 9$ to 10). (B, C, D and E) Representative images of PAS staining (B), Masson trichrome staining (C), immunostaining for COL1A1 (D), and ADGRE1/F4/80 (E) in the kidney cortical regions of obese CTRL, *atg5*$^{F/F}$-TSKO, and TSDKO mice ($n = 4$ to 6) under a high-fat diet for 10 months. The tubular injury score (B right), COL1A1-positive area (D right), and ADGRE1/F4/80-positive area (E right) were quantified in at least 10 high-power fields (×400), respectively. Kidney sections were counterstained with hematoxylin. Bars: 50 m. Data are provided as means ± SE. Statistically significant differences (*$P < 0.05$) are indicated.

and AMPK [56,57], whereas endogenous FGF21 in PTECs may be necessary to maintain energy homeostasis and/or reduce oxidative stress, and thus suppress aberrant autophagy. In other words, endogenous FGF21 May be coordinated with autophagy to maintain homeostasis. This notion is also supported by previous studies showing that autophagy is coordinated with other cellular activities to maintain homeostasis and is upregulated in a compensatory manner when the ubiquitin – proteasome system or chaperone-mediated autophagy is compromised [59,60].

PTEC-specific *fgf21* deletion per se is not sufficient to lead to CKD progression in *young* mice, presumably because endogenous FGF21 in PTECs appears to play a dispensable role under basal conditions and enhanced autophagy plays a compensatory role. Constitutive up-regulation of autophagy is unable, however, to compensate for all functions of endogenous FGF21. Not only that, considering that aging and obesity lead to higher basal autophagic flux along with stagnation at later stage which jeopardize tubular functions, *fgf21* deletion accompanied by excessive autophagy can place

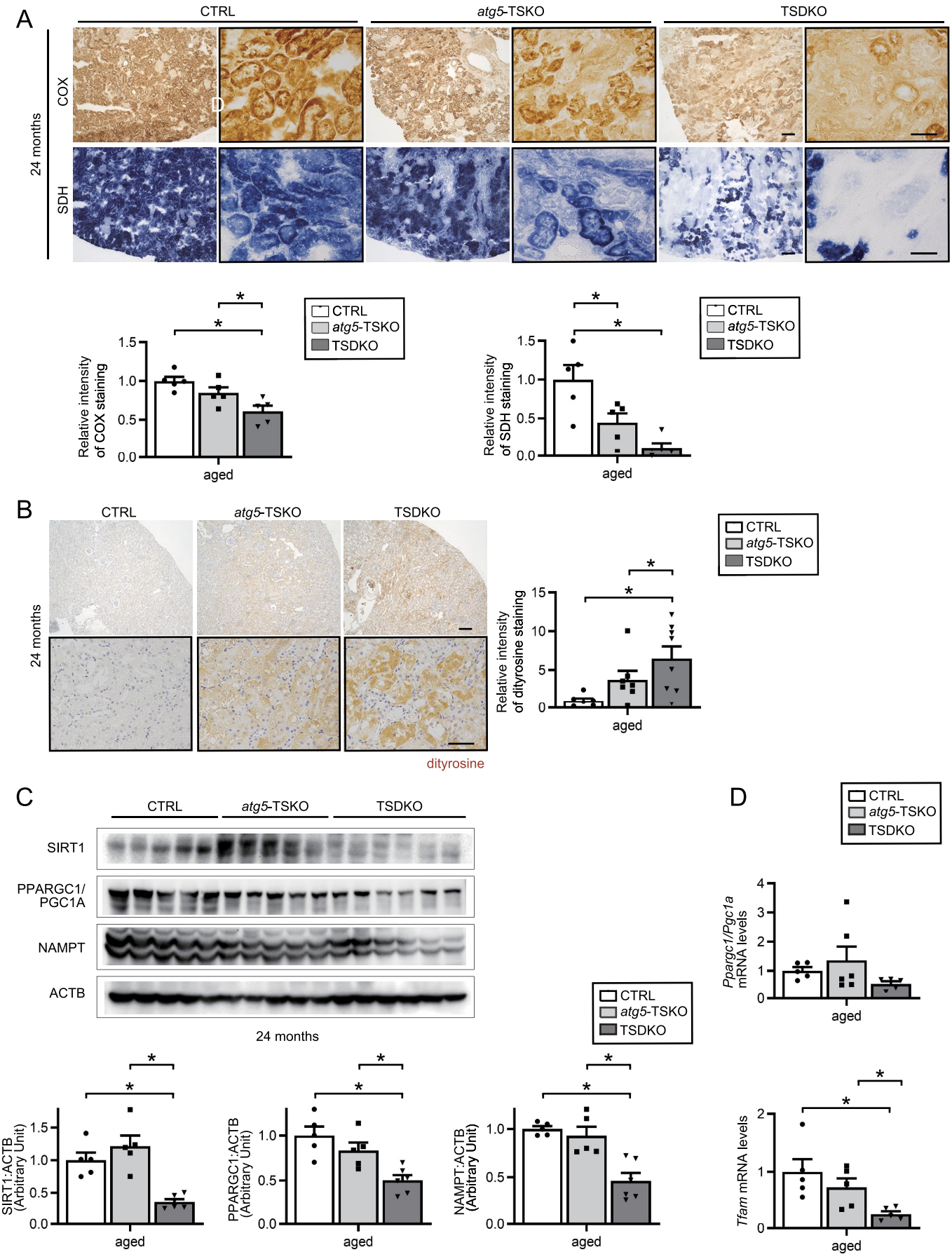

Figure 7. FGF21 deficiency accelerates kidney aging with mitochondrial dysfunction and oxidative stress. (A and B) Representative images of immunostaining for COX and SDH staining (A), and dityrosine (B) in the kidney cortical regions of aged CTRL, *atg5*$^{F/F}$-TSKO, and TSDKO mice ($n = 5$ (A), and 5 to 8 (B)). Magnified images

a greater burden on lysosomal system and enhance the susceptibility of mice to the development of CKD progression during aging and obesity. Furthermore, autophagy stagnation predisposes PTECs to AKI [9]. We speculate that FGF21 resistance coupled to stagnation of autophagy in the kidney of elderly and obese individuals might contribute to the increased susceptibility to and severity of pathologies including AKI, maladaptive repair, and the subsequent development of CKD, which remains to be elucidated in more detail.

Our observation that FGF21 deficiency accelerates CKD progression with oxidative stress and mitochondrial dysfunction in autophagy-deficient mice kidneys indicates that FGF21 reduces oxidative stress and maintains mitochondrial homeostasis irrespective of autophagy/mitophagy. Consistently, recent studies have reported that FGF21 induces the expression of genes involved in antioxidative pathways, including UCP2 (uncoupling protein 2 (mitochondrial, proton carrier)) and UCP3 and SOD2 (superoxide dismutase-2) [61] and that FGF21 improves mitochondrial biogenesis/dynamics [62,63]. Importantly, the following are reported so far in relation to the molecular mechanisms by which FGF21 functions in the maintenance of mitochondrial oxidative stress. First, FGF21 counteracts oxidative stress during cellular senescence [36] and cardiac hypertrophy [64] in a SIRT1-dependent manner. Second, SIRT1 maintains mitochondrial function via the PPARGC1A/PGC1A-TFAM pathway, i.e., SIRT1 activates PPARGC1A/PGC1A by deacetylating it, and the activated PPARGC1A/PGC1A promotes transcription of TFAM [38,39], which is important for the maintenance of mitochondrial integrity. Indeed, SIRT1 protein levels and *Tfam* transcription were markedly decreased in the kidney of aged TSDKO mice compared to *aged atg5*$^{F/F}$-TSKO mice (Figure 7D). Furthermore, recent reports have elucidated that TFAM in PTECs is essential for kidney homeostasis by maintaining mitochondrial function [54,55]. Taken together, FGF21 May counter the progression of CKD by maintaining mitochondrial homeostasis partly through the SIRT1-PPARGC1A/PGC1A-TFAM pathway, although further molecular validation is needed in the future.

While several reports have shown that FGF21 activates SIRT1 [36,37,65], it is still unclear why SIRT1 is activated by FGF21. In this study, we examined the expression of NAMPT, a rate-limiting enzyme for NAD^+ synthesis, which is essential for SIRT1 activation, and found that NAMPT expression was also decreased in the kidney of aged TSDKO mice (Figure 7C). Conversely, AMPK, an important activator of NAMPT and SIRT1 [40], was rather activated in aged TSDKO mice (Figure S5C), suggesting that the decreased expression of NAMPT and SIRT1 in the kidney of aged TSDKO mice is AMPK-independent. The detailed mechanism by which FGF21 activates NAMPT and SIRT1 requires further investigation in the future.

In conclusion, we report that FGF21 is robustly induced by autophagy disturbance to protect against CKD progression by maintaining mitochondrial homeostasis during aging and obesity, which will pave the way to a novel treatment of CKD.

Materials and methods

Mice

Kap-Cre mice, GFP-MAP1LC3B transgenic mice, *Atg5*-floxed mice [7], and EGFP-ChAT mice [32] all with a C57BL/6N background were as described previously. *Fgf21*-floxed mice was originally obtained from the Jackson Laboratory (Bar Harbor, ME, USA). To generate *Fgf21*-floxed *Kap*-Cre mice (*fgf21*$^{F/F}$-TSKO mice), *Fgf21*-floxed mice, in which exons 1–3 of the *Fgf21* gene is flanked by two lox P sequences, were crossed with the *Kap*-Cre transgenic mice. To generate PTEC-specific *fgf21*- and *atg5*-deficient mice (*fgf21* $^{F/F}$ *atg5* $^{F/F}$-TSDKO mice), *Fgf21*-floxed mice were crossed with *atg5* $^{F/F}$-TSKO mice. All mice were housed in box cages, maintained on a 12-h light/12-h dark cycle. *In vivo* autophagy flux assay using chloroquine (Sigma-Aldrich, C6628) were described previously [8]. For studying the effects of HFD-induced obesity, eight-week-old mice were fed an ND (12.8% of kcal from fat: 5% fat, 23% protein, and 55% carbohydrate) or HFD (62.2% of kcal from fat: 35% fat, 23% protein, and 25% carbohydrate) (Oriental Yeast, HFD-60) for 2 or 10 months. All animal experiments were approved by the institutional committees of the Animal Research Committee of Osaka University and conformed to the Japanese Animal Protection and Management Law (No.25).

Antibodies and reagents

We used the following antibodies; LRP2/MEGALIN (low density lipoprotein receptor-related protein 2) (a gift from Dr. Michigami, Department of Bone and Mineral Research, Osaka Medical Center and Research Institute for Maternal and Child Health, Osaka, Japan), LAMP1 (BD Biosciences, 553792), SQSTM1/p62 (Medical and Biologic Laboratory, PM045 for western blotting, Progen, GP62-C for immunostaining), ubiquitin (Cell Signaling Technology, 3936), COL1A1 (Abcam, ab34710), ADGRE1/F4/80 (BIO-RAD, MCA497), CDKN1A/p21^{cip1} (Abcam, ab109199), phospho-H2AFX/γ-H2AX (Ser139; EMD Millipore, 05–636-I), dityrosine (Japan Institute for the Control of Aging, MDT-020P), 4HNE (Japan Institute for the Control of Aging, MHN-020P), CML (Transgenic, KH024), phosphorylated PRKAA/AMPK Cell Signaling Technology, 2535), AMPK (Cell Signaling Technology, 2532), phosphorylated RPS6 (Ser235/236; Cell Signaling Technology, 2211), NAMPT (Bethyl Laboratories, A300-372A), SIRT1 (EMD Millipore, 07–131), PPARGC1A/

are presented in the insets (A). Kidney sections were counterstained with hematoxylin (B). The relative intensity was quantified in at least 10 high-power fields (×400), respectively. Bars: 50 m. (C) mRNA expression levels of *Ppargc1a/Pgc1a* and *Tfam* using whole kidney lysates of *aged* CTRL, *atg5*$^{F/F}$-TSKO, and TSDKO mice (n = 5 to 6). Data were normalized with *Gapdh* mRNA. (D) Representative immunoblot and quantification by densitometry of the protein level of SIRT1, PPARGC1/PGC1A and NAMPT using whole kidney lysates of *aged* CTRL, *atg5*$^{F/F}$-TSKO, and TSDKO mice are shown (n = 5 to 6). ACTB was used as loading control. Data are expressed as the fold change relative to the mean value of aged CTRL mice and are provided as means ± SE. Statistically significant differences (*P < 0.05) are indicated.

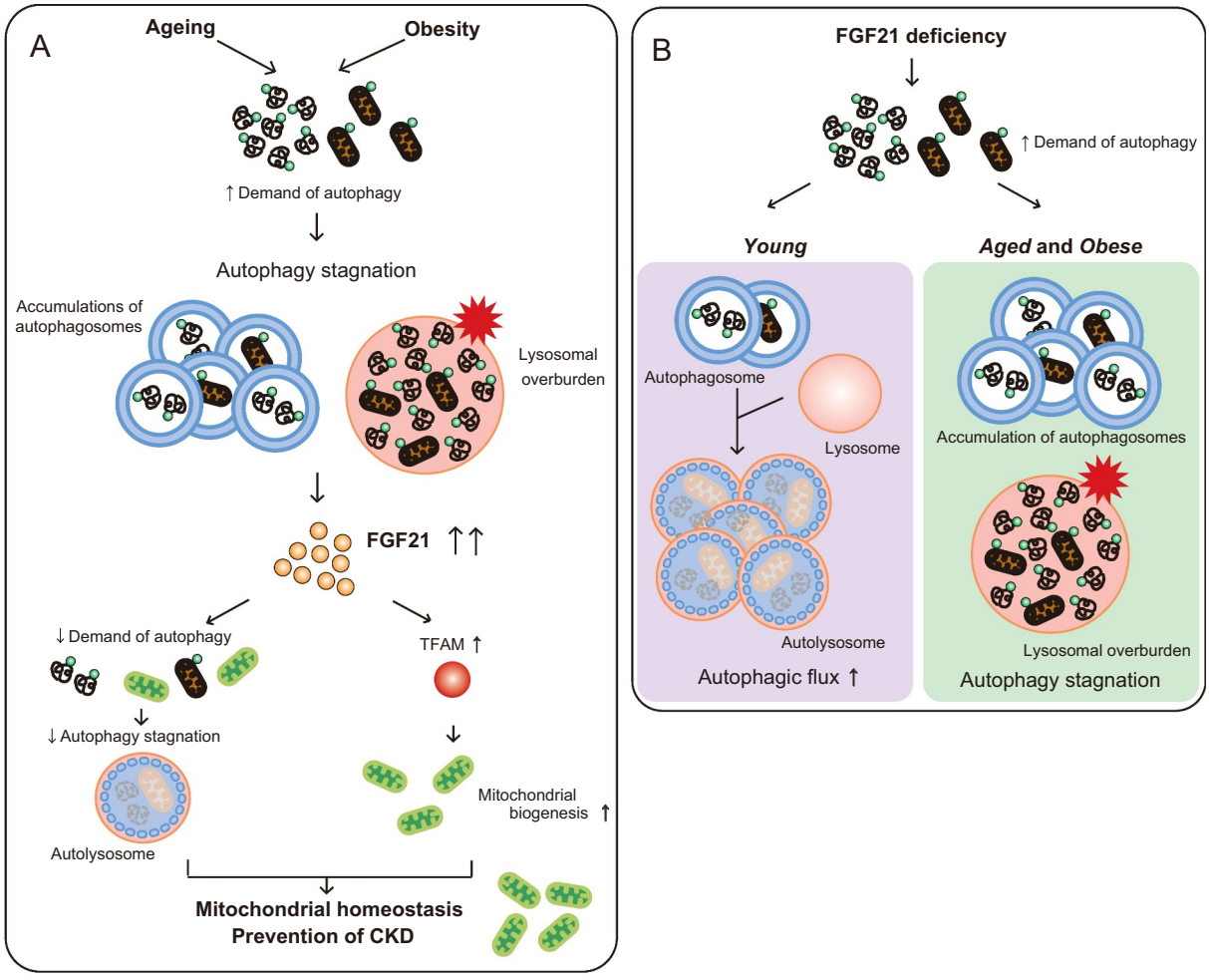

Figure 8. FGF21 is robustly induced by autophagy disturbance to protect against CKD progression during aging and obesity. (A) endogenous FGF21 is significantly induced under autophagy stagnation, and protects against age- and obesity-related CKD progression by alleviating autophagy stagnation and maintaining mitochondrial homeostasis. (B) There exists an apparent interaction between FGF21 and autophagy in PTECs; FGF21 deficiency increases the demand of autophagy, leading to the increased autophagic flux in *young* mice while autophagy is stagnated due to lysosomal overburden in aged and obese kidney.

PGC1A (Abcam, ab54481), ACTB (Sigma-Aldrich, A5316), biotinylated secondary antibodies (Vector Laboratories, BA-1000 [anti-rabbit IgG], BA-2001 [anti-mouse IgG], BA-4000 [anti-rat IgG], BA-7000 [anti-guinea pig IgG]), horseradish peroxidase-conjugated secondary antibodies (DAKO, P0448 [anti-rabbit IgG], P0447 [anti-mouse IgG]), and Alexa Fluor-conjugated secondary antibody (Invitrogen, A31572 [anti-rabbit Alexa Fluor 555], A21434 [anti-rat Alexa Fluor 555]).

Histologic analysis

Histological analysis was performed as described previously with modification [8]. Antigen retrieval on paraffin-embedded sections, double staining for SQSTM1/p62 (or ubiquitin) and LRP2/MEGALIN, quantifying the percentage of the COL1A1 (or Sirius red, ADGRE1/F4/80, dityrosine, 4HNE, CML)-positive area, electron microscopy analysis, Masson trichrome-, Nile red-, and COX/SDH- staining, quantifying the percentage of fibrotic area were described previously [8,9]. The tubular injury score and the vacuole score were assessed using PAS-stained sections. Tubular injury was defined by loss of brush border, cytosolic vacuolar formation, tubular lumen dilation and tubular atrophy, and kidney tubular cells of the cortex were scored from 0 to 10 according to the percentage of injured tubules. Tubular vacuolation was graded semiquantitatively from 0 to 10 according to the percentage of vacuolated tubules as described previously [66]. In all quantitative or semiquantitative analysis of histological staining, at least 10 high-power fields were reviewed for each tissue by two nephrologists (A.T. and T.N-H.) in a blinded manner.

Biochemical parameters

Blood samples were collected from mice under anesthesia. Plasma was obtained after centrifugation (15 min, 845 ×g, 4°C) and concentrations of urea nitrogen, creatinine, cystatin C, glucose, total cholesterol, triglycerides, free fatty acids, phospholipids, FGF21 were measured using the BUN-Test-Wako (Wako, 279–36201), the CRE-EN Kainos (Kainos, TKA7500), cystatin C (mouse) ELISA kit (BioVendor, RD291009200R), the Glucose CII-test (Wako, 439–90901),

the Cholesterol E-test (Wako, 439–17501), the Triglyceride E-test (Wako, 432–40201), the NEFA C-test (Wako, 279–75401), the Phospholipid C-test (Wako, 433–36201), and the Mouse/Rat FGF21 Quantikine ELISA Kit (R&D Systems, MF2100). Urinary albumin excretion was measured with the Microfluoral^{TM} microalbumin test (Progen, PR2005). All kits were used in accordance with the manufacturer's protocols.

Quantitative RT-PCR and western blot analysis

Quantitative RT-PCR and western blot analyses were performed as described previously [67]. The sequences of the primers used were as follows: *Fgf21*-F, 5′-tacacagatgacgaccaaga-3′; *Fgf21*-R, 5′-ggcttcagactggtacacat-3′; *Sqstm1/p62*-F, 5′-atgtgcatatgctgacgcct-3′; *Sqstm1/p62*-R, 5′- caggcctagggaaagcagag-3′; *Havcr1*-F, 5′-tcagct cgggaatgcaca-3′; *Havcr1*-R, 5′-tggttgccttccgtgtct-3′; *Lcn2*-F, 5′-ctacaaccagttcgccatgg-3′; *Lcn2*-R, 5′-acactcaccacccattcagt-3′; *Col 1a1*-F, 5′-acgccatcaaggtctactgc-3′; *Col1a1*-R, 5′-actcgaacgggaat ccatcg-3′; *Tgfb* (transforming growth factor beta)-F, 5′-ttgcttcag ctccacagaga-3′; *Tgfb*-R, 5′-tggttgtagagggcaaggac-3′; *Cdkn2a/ p19^{Arf}*-F, 5′-gcaggttcttggtcactgtg-3′; *Cdkn2a/p19^{Arf}*-R, 5′-gatcg cacgaacttcaccaa-3′; *Ppargc1a/Pgc1a*-F, 5′-atgtgtcgccttcttgctct-3′; *Ppargc1a/Pgc1a* -R, 5′-atgtagtgcctggggacctt-3′; *Tfam*-F, 5′-gagc agctaactccaagtcag-3′; *Tfam*-R, 5′-gagccgaatcatcctttgcct-3′; Atf4 (activating transcription factor 4)-F, 5′-ccttcgaccagtcgggtttg-3′; *Atf4*-R, 5′-ctgtcccggaaaaggcatcc-3′; *Ddit3/Chop* (DNA damage inducible transcript 3)-F, 5′-gaagcctggtatgaggatct-3′; *Ddit3/ Chop*-R, 5′-actgaccactctgtttccgt-3′; *Hspa5/Bip* (heat shock protein 5)-F, 5′-ctgggtacatttgatctgactgg-3′; *Hspa5/Bip*-R, 5′-gcatcct ggtggctttccagccat-3′; *Dnajb9/Erdj4* (DnaJ heat shock protein family (Hsp40) member B9)-F, 5′-gaattaatcctggcctccaa-3′; *Dnajb9/Erdj4*-R, 5′-cagggtggtacttcatggct-3′; *Xbp1s* (X-box binding protein 1; spliced form)-F, 5′-gagtccgcagcaggtg-3′; *Xbp1s*-R, 5′-gtgtcagagtccatggga-3′; *Gapdh* (glyceraldehyde-3-phosphate dehydrogenase)-F, 5′- aactttggcattgtggaagg –3′; *Gapdh*-R, 5′-acacattgggggtaggaaca –3′.

Statistical analysis

All results are presented as means ± standard error (SE). Statistical analyses were conducted using GraphPad Prism 7 software (GraphPad software). As appropriate, statistical analysis was performed using unpaired Student-t-test, oneway or two-way analysis of variance (ANOVA) followed by Student-Newman-Keuls post hoc test, or Kruskal Wallis test followed by Dunn's multiple comparison post hoc test. Statistical significance was defined as $P < 0.05$.

Abbreviations

ACTB	actin, beta
ADGRE1/F4/80	adhesion G protein-coupled receptor E1
AKI	acute kidney injury
AMPK	AMP-activated protein kinase
ATF4	activating transcription factor 4
ATG	autophagy related
ChAT	chloramphenicol acetyltransferase
CDKN1A/p21^{cip1}	cyclin dependent kinase inhibitor 1A
CDKN2A/p19^{Arf}	cyclin dependent kinase inhibitor 2A
CKD	chronic kidney disease
CML	N-carboxymethyllysine
COL1A1	Collagen, type I, alpha 1
COX	cytochrome c oxidase
CRE	creatinine
CTRL	control
DDIT3/CHOP	DNA-damage inducible transcript 3
DNAJB9/ERDJ4	DnaJ heat shock protein family (Hsp40) member B9
EGFP	enhanced green fluorescent protein
ER	endoplasmic reticulum
FGF21	fibroblast growth factor 21
GAPDH	glyceraldehyde-3-phosphate dehydrogenase
GFP	green fluorescent protein
HAVCR1/KIM-1	hepatitis A virus cellular receptor 1
HFD	high-fat diet
HNE	4-hydroxy-2-nonenal
HSPA5/BIP	heat shock protein 5
KAP	kidney androgen regulated protein
LAMP1	lysosomal-associated membrane protein 1
LCN2/NGAL	lipocalin 2
LRP2	low density lipoprotein receptor-related protein 2
MAP1LC3B/LC3	microtubule-associated protein 1 light chain 3 beta
mitoISR	mitochondrial integrated stress response
MTORC1	mechanistic target of rapamycin kinase complex 1
NAD	nicotinamide adenine dinucleotide
NAMPT	nicotinamide phosphoribosyltransferase
PAS	periodic-acid schiff
PPARGC1/PGC1	peroxisome proliferative activated receptor, gamma, coactivator 1
PTEC	proximal tubular epithelial cell
ROS	reactive oxygen species
RPS6	ribosomal protein S6
SDH	succinate dehydrogenase complex
SIRT1	sirtuin 1
SOD	superoxide dismutase
SQSTM1/p62	sequestosome 1
TFAM	transcription factor A, mitochondrial
TGFB/TGFβ	transforming growth factor, beta
TSDKO	tissue-specific double knockout
TSKO	tissue-specific knockout
UCP	uncoupling protein (mitochondrial, proton carrier)
phospho-H2AFX/γ-H2AX	phosphorylated H2A.X variant histone
XBP1s	X-box binding protein 1; spliced form

Acknowledgements

We thank N. Mizushima, University of Tokyo, for *Atg5$^{F/F}$* and GFP-MAP1LC3B mice; T. Matsusaka and F. Niimura, Tokai University School of Medicine, for *KAP-Cre* mice; T. Michigami, Osaka Medical Center and Research Institute, for LRP2/MEGALIN antibody; and N. Horimoto for technical assistance.

Disclosure statement

No potential conflict of interest was reported by the authors.

Funding

This work was supported by a Grant-in-Aid for Scientific Research from the Ministry of Education, Culture, Sports, Science and Technology in Japan (17K16082 [to S.Minami], 19K17741 [to S.S.],17K16083 and 21K16163 [to T.Y.], 15K09260 and 18K08208 [to Y.T.], and 17H04188 [to Y.I.]), Japan Agency for Medical Research and Development (AMED) (JP22gm1410014 [to Y.I., S.Minami, and T.Y.]), the Project MEET, Osaka University Graduate School of Medicine (to S.Minami), the Mitsubishi Tanabe Pharma Corporation (to S.Minami), and Bayer Academic Support (to T.Y.).

References

[1] Jager KJ, Kovesdy C, Langham R, et al. A single number for advocacy and communication-worldwide more than 850 million individuals have kidney diseases. Kidney Int. 2019 Nov;96 (5):1048–1050. doi: 10.1016/j.kint.2019.07.012

[2] Global, regional, and znational age-sex specific all-cause and cause-specific mortality for 240 causes of death, 1990-2013: A systematic analysis for the global burden of disease study 2013. Lancet. 2015 Jan 10;385(9963):117–171. doi: 10.1016/S0140-6736(14)61682-2

[3] Rhee CM, CP K. Epidemiology: spotlight on CKD deaths—increasing mortality worldwide. Nat Rev Nephrol. 2015 Apr;11 (4):199–200. doi: 10.1038/nrneph.2015.25

[4] Breyer MD, Susztak K. The next generation of therapeutics for chronic kidney disease. Nat Rev Drug Discov. 2016 Aug;15 (8):568–588. doi: 10.1038/nrd.2016.67

[5] Little MH, Humphreys BD. Regrow or repair: an update on potential regenerative therapies for the kidney. J Am Soc Nephrol. 2022 Jan;33(1):15–32. doi: 10.1681/ASN.2021081073

[6] Mizushima N, Levine B, Cuervo AM, et al. Autophagy fights disease through cellular self-digestion. Nature. 2008 Feb 28;451 (7182):1069–1075. doi: 10.1038/nature06639

[7] Kimura T, Takabatake Y, Takahashi A, et al. Autophagy protects the proximal tubule from degeneration and acute ischemic injury. J Am Soc Nephrol. 2011 May;22(5):902–913. doi: 10.1681/ASN.2010070705

[8] Yamamoto T, Takabatake Y, Kimura T, et al. Time-dependent dysregulation of autophagy: implications in aging and mitochondrial homeostasis in the kidney proximal tubule. Autophagy. 2016 May 3;12(5):801–813. doi: 10.1080/15548627.2016.1159376

[9] Yamamoto T, Takabatake Y, Takahashi A, et al. High-fat diet-induced lysosomal dysfunction and impaired autophagic flux contribute to lipotoxicity in the kidney. J Am Soc Nephrol. 2017 May;28(5):1534–1551. doi: 10.1681/ASN.2016070731

[10] Takahashi A, Takabatake Y, Kimura T, et al. Autophagy inhibits the accumulation of advanced glycation end products by promoting lysosomal biogenesis and function in the kidney proximal tubules. Diabetes. 2017 May;66(5):1359–1372. doi: 10.2337/db16-0397

[11] Sakai S, Yamamoto T, Takabatake Y, et al. Proximal tubule autophagy differs in type 1 and 2 Diabetes. J Am Soc Nephrol. 2019 Jun;30(6):929–945. doi: 10.1681/ASN.2018100983

[12] Bordi M, Berg MJ, Mohan PS, et al. Autophagy flux in CA1 neurons of alzheimer hippocampus: increased induction overburdens failing lysosomes to propel neuritic dystrophy. Autophagy. 2016 Dec;12(12):2467–2483. doi: 10.1080/15548627.2016.1239003

[13] Takabatake Y, Yamamoto T, Isaka Y. Stagnation of autophagy: a novel mechanism of renal lipotoxicity. Autophagy. 2017 Apr 3;13(4):775–776. doi: 10.1080/15548627.2017.1283084

[14] Yamamoto T, Takabatake Y, Minami S, et al. Eicosapentaenoic acid attenuates renal lipotoxicity by restoring autophagic flux. Autophagy. 2021 Jul;17(7):1700–1713. doi: 10.1080/15548627.2020.1782034

[15] Yamamoto-Imoto H, Minami S, Shioda T, et al. Age-associated decline of MondoA drives cellular senescence through impaired autophagy and mitochondrial homeostasis. Cell Rep. 2022 Mar 1;38(9):110444. doi: 10.1016/j.celrep.2022.110444

[16] Kharitonenkov A, DiMarchi R. Fibroblast growth factor 21 night watch: advances and uncertainties in the field. J Intern Med. 2017 Mar;281(3):233–246. doi: 10.1111/joim.12580

[17] Xie T, Leung PS. Fibroblast growth factor 21: a regulator of metabolic disease and health span. Am J Physiol Endocrinol Metab. 2017 Sep 1;313(3):E292–E302. doi: 10.1152/ajpendo.00101.2017

[18] Ye D, Wang Y, Li H, et al. Fibroblast growth factor 21 protects against acetaminophen-induced hepatotoxicity by potentiating peroxisome proliferator-activated receptor coactivator protein-1alpha-mediated antioxidant capacity in mice. Hepatology. 2014 Sep;60(3):977–989. doi: 10.1002/hep.27060

[19] Kim SH, Kim KH, Kim HK, et al. Fibroblast growth factor 21 participates in adaptation to endoplasmic reticulum stress and attenuates obesity-induced hepatic metabolic stress. Diabetologia. 2015 Apr;58(4):809–818. doi: 10.1007/s00125-014-3475-6

[20] Hojman P, Pedersen M, Nielsen AR, et al. Fibroblast growth factor-21 is induced in human skeletal muscles by hyperinsulinemia. Diabetes. 2009 Dec;58(12):2797–2801. doi: 10.2337/db09-0713

[21] Kim KH, Jeong YT, Oh H, et al. Autophagy deficiency leads to protection from obesity and insulin resistance by inducing Fgf21 as a mitokine. Nat Med. 2013 Jan;19(1):83–92. doi: 10.1038/nm.3014

[22] Planavila A, Redondo I, Hondares E, et al. Fibroblast growth factor 21 protects against cardiac hypertrophy in mice. Nat Commun. 2013;4(1):2019. doi: 10.1038/ncomms3019

[23] Salminen A, Kaarniranta K, Kauppinen A. Regulation of longevity by FGF21: interaction between energy metabolism and stress responses. Ageing Res Rev. 2017 May 25;37:79–93. doi: 10.1016/j.arr.2017.05.004

[24] Youm YH, Horvath TL, Mangelsdorf DJ, et al. Prolongevity hormone FGF21 protects against immune senescence by delaying age-related thymic involution. Proc Natl Acad Sci U S A. 2016 Jan 26;113(4):1026–1031. doi: 10.1073/pnas.1514511113

[25] Jimenez V, Jambrina C, Casana E, et al. FGF21 gene therapy as treatment for obesity and insulin resistance. EMBO Mol Med. 2018 Aug;10(8):e8791. doi: 10.15252/emmm.201708791

[26] Zhang Y, Xie Y, Berglund ED, et al. The starvation hormone, fibroblast growth factor-21, extends lifespan in mice. Elife. 2012 Oct 15;1:e00065. doi: 10.7554/eLife.00065

[27] Kim HW, Lee JE, Cha JJ, et al. Fibroblast growth factor 21 improves insulin resistance and ameliorates renal injury in db/db mice. Endocrinology. 2013 Sep;154(9):3366–3376. doi: 10.1210/en.2012-2276

[28] Zhang C, Shao M, Yang H, et al. Attenuation of hyperlipidemia- and diabetes-induced early-stage apoptosis and late-stage renal dysfunction via administration of fibroblast growth factor-21 is associated with suppression of renal inflammation. PLoS One. 2013;8(12):e82275. doi: 10.1371/journal.pone.0082275

[29] Minami S, Yamamoto T, Takabatake Y, et al. Lipophagy maintains energy homeostasis in the kidney proximal tubule during prolonged starvation. Autophagy. 2017 Oct 3;13(10):1629–1647. doi: 10.1080/15548627.2017.1341464

[30] Loeffler I, Hopfer U, Koczan D, et al. Type VIII collagen modulates TGF-β1-induced proliferation of mesangial cells. J Am Soc Nephrol. 2011 Apr;22(4):649–663. doi: 10.1681/ASN.2010010098

[31] Li F, Liu Z, Tang C, et al. FGF21 is induced in cisplatin nephrotoxicity to protect against kidney tubular cell injury. FASEB J. 2018 Jun;32(6):3423–3433. doi: 10.1096/fj.201701316R

[32] Kawamoto S, Niwa H, Tashiro F, et al. A novel reporter mouse strain that expresses enhanced green fluorescent protein upon Cre-mediated recombination. FEBS Lett. 2000 Mar 31;470 (3):263–268. doi: 10.1016/S0014-5793(00)01338-7

[33] Docherty MH, O'Sullivan ED, Bonventre JV, et al. Cellular senescence in the kidney. J Am Soc Nephrol. 2019 May;30(5):726–736. doi: 10.1681/ASN.2018121251

[34] Tang C, Cai J, Yin XM, et al. Mitochondrial quality control in kidney injury and repair. Nat Rev Nephrol. 2021 May;17 (5):299–318. doi: 10.1038/s41581-020-00369-0

[35] Cybulsky AV. Endoplasmic reticulum stress, the unfolded protein response and autophagy in kidney diseases. Nat Rev Nephrol. 2017 Nov;13(11):681–696. doi: 10.1038/nrneph.2017.129
[36] Yan J, Wang J, Huang H, et al. Fibroblast growth factor 21 delayed endothelial replicative senescence and protected cells from H(2)O(2)-induced premature senescence through SIRT1. Am J Transl Res. 2017;9(10):4492–4501.
[37] Chen Q, Ma J, Yang X, et al. SIRT1 mediates effects of FGF21 to ameliorate cisplatin-induced acute kidney injury. Front Pharmacol. 2020;11:241. doi: 10.3389/fphar.2020.00241
[38] Yuan X, Wei G, You Y, et al. Rutin ameliorates obesity through brown fat activation. FASEB J. 2017 Jan;31(1):333–345. doi: 10.1096/fj.201600459rr
[39] Zhang C, He X, Sheng Y, et al. Allicin regulates energy homeostasis through brown adipose tissue. iScience. 2020 May 22;23(5):101113. doi: 10.1016/j.isci.2020.101113
[40] Canto C, Gerhart-Hines Z, Feige JN, et al. AMPK regulates energy expenditure by modulating NAD+ metabolism and SIRT1 activity. Nature. 2009 Apr 23;458(7241):1056–1060. doi: 10.1038/nature07813
[41] Croon M, Szczepanowska K, Popovic M, et al. FGF21 modulates mitochondrial stress response in cardiomyocytes only under mild mitochondrial dysfunction. Sci Adv. 2022 Apr 8;8(14):eabn7105. doi: 10.1126/sciadv.abn7105
[42] McWilliams TG, Prescott AR, Allen GF, et al. Mito-QC illuminates mitophagy and mitochondrial architecture in vivo. J Cell Bio. 2016 Aug 1;214(3):333–345. doi: 10.1083/jcb.201603039
[43] Ishii K, Kobayashi H, Taguchi K, et al. Kidney epithelial targeted mitochondrial transcription factor a deficiency results in progressive mitochondrial depletion associated with severe cystic disease. Kidney Int. 2021 Mar;99(3):657–670. doi: 10.1016/j.kint.2020.10.013
[44] Chung KW, Dhillon P, Huang S, et al. Mitochondrial damage and activation of the STING pathway lead to renal inflammation and fibrosis. Cell Metab. 2019 Oct 1;30(4):784–799 e5. doi: 10.1016/j.cmet.2019.08.003
[45] Fisher FM, Chui PC, Antonellis PJ, et al. Obesity is a fibroblast growth factor 21 (FGF21)-resistant state. Diabetes. 2010 Nov;59(11):2781–2789. doi: 10.2337/db10-0193
[46] So WY, Cheng Q, Chen L, et al. High glucose represses β-klotho expression and impairs fibroblast growth factor 21 action in mouse pancreatic islets: involvement of peroxisome proliferator-activated receptor γ signaling. Diabetes. 2013 Nov;62(11):3751–3759. doi: 10.2337/db13-0645
[47] Díaz-Delfín J, Hondares E, Iglesias R, et al. TNF-α represses β-Klotho expression and impairs FGF21 action in adipose cells: involvement of JNK1 in the FGF21 pathway. Endocrinology. 2012 Sep;153(9):4238–4245. doi: 10.1210/en.2012-1193
[48] Hanks LJ, Gutiérrez OM, Bamman MM, et al. Circulating levels of fibroblast growth factor-21 increase with age independently of body composition indices among healthy individuals. J Clin Transl Endocrinol. 2015 Jun 1;2(2):77–82. doi: 10.1016/j.jcte.2015.02.001
[49] Xia S, Zhang X, Zheng S, et al. An update on inflamm-aging: mechanisms, prevention, and treatment. J Immunol Res. 2016;2016:8426874. doi: 10.1155/2016/8426874
[50] Stein S, Bachmann A, Lössner U, et al. Serum levels of the adipokine FGF21 depend on renal function. Diabetes Care. 2009 Jan;32(1):126–128. doi: 10.2337/dc08-1054
[51] Lin Z, Zhou Z, Liu Y, et al. Circulating FGF21 levels are progressively increased from the early to end stages of chronic kidney diseases and are associated with renal function in Chinese. PLoS One. 2011;6(4):e18398. doi: 10.1371/journal.pone.0018398
[52] Hindricks J, Ebert T, Bachmann A, et al. Serum levels of fibroblast growth factor-21 are increased in chronic and acute renal dysfunction. Clin Endocrinol (Oxf). 2014 Jun;80(6):918–924. doi: 10.1111/cen.12380
[53] Lee CH, Hui EY, Woo YC, et al. Circulating fibroblast growth factor 21 levels predict progressive kidney disease in subjects with type 2 diabetes and normoalbuminuria. J Clin Endocrinol Metab. 2015 Apr;100(4):1368–1375. doi: 10.1210/jc.2014-3465
[54] Ruperez C, Lerin C, Ferrer-Curriu G, et al. Autophagic control of cardiac steatosis through FGF21 in obesity-associated cardiomyopathy. Int J Cardiol. 2018 Jun 1;260:163–170. doi: 10.1016/j.ijcard.2018.02.109
[55] Zhu S, Wu Y, Ye X, et al. FGF21 ameliorates nonalcoholic fatty liver disease by inducing autophagy. Mol Cell Biochem. 2016 Sep;420(1–2):107–119. doi: 10.1007/s11010-016-2774-2
[56] Cheng STW, SYT L, Leung PS. Fibroblast growth factor 21 stimulates pancreatic islet autophagy via inhibition of AMPK-mTOR signaling. Int J Mol Sci. 2019 May 22;20(10):2517. doi: 10.3390/ijms20102517
[57] Zhou K, Chen H, Lin J, et al. FGF21 augments autophagy in random-pattern skin flaps via AMPK signaling pathways and improves tissue survival. Cell Death Dis. 2019 Nov 18;10(12):872. doi: 10.1038/s41419-019-2105-0
[58] Zhang J, Cheng Y, Gu J, et al. Fenofibrate increases cardiac autophagy via FGF21/SIRT1 and prevents fibrosis and inflammation in the hearts of type 1 diabetic mice. Clin Sci. 2016 Apr;130(8):625–641. doi: 10.1042/CS20150623
[59] Pandey UB, Nie Z, Batlevi Y, et al. HDAC6 rescues neurodegeneration and provides an essential link between autophagy and the UPS. Nature. 2007 Jun 14;447(7146):859–863. doi: 10.1038/nature05853
[60] Massey AC, Kaushik S, Sovak G, et al. Consequences of the selective blockage of chaperone-mediated autophagy. Proc Natl Acad Sci U S A. 2006 Apr 11;103(15):5805–5810. doi: 10.1073/pnas.0507436103
[61] Planavila A, Redondo-Angulo I, Ribas F, et al. Fibroblast growth factor 21 protects the heart from oxidative stress. Cardiovasc Res. 2015 Apr 1;106(1):19–31. doi: 10.1093/cvr/cvu263
[62] Wang XM, Xiao H, Liu LL, et al. FGF21 represses cerebrovascular aging via improving mitochondrial biogenesis and inhibiting p53 signaling pathway in an AMPK-dependent manner. Exp Cell Res. 2016 Aug 15;346(2):147–156. doi: 10.1016/j.yexcr.2016.06.020
[63] Li X, Hong Y, He H, et al. FGF21 mediates mesenchymal stem Cell senescence via Regulation of mitochondrial Dynamics. Oxid Med Cell Longev. 2019;2019:4915149. doi: 10.1155/2019/4915149
[64] Li S, Zhu Z, Xue M, et al. Fibroblast growth factor 21 protects the heart from angiotensin II-induced cardiac hypertrophy and dysfunction via SIRT1. Biochim Biophys Acta Mol Basis Dis. 2019 Jun 1;1865(6):1241–1252. doi: 10.1016/j.bbadis.2019.01.019
[65] Liu X, Wang Y, Hou L, et al. Fibroblast growth factor 21 (FGF21) promotes formation of aerobic myofibers via the FGF21-SIRT1-AMPK-PGC1alpha pathway. J Cell Physiol. 2017 Jul;232(7):1893–1906. doi: 10.1002/jcp.25735
[66] Nakamura J, Yamamoto T, Takabatake Y, et al. TFEB-mediated lysosomal exocytosis alleviates high-fat diet-induced lipotoxicity in the kidney. JCI Insight. 2023 Feb 22;8(4). doi: 10.1172/jci.insight.162498
[67] Matsui I, Ito T, Kurihara H, et al. Snail, a transcriptional regulator, represses nephrin expression in glomerular epithelial cells of nephrotic rats. Lab Invest. 2007 Mar;87(3):273–283. doi: 10.1038/labinvest.3700518